Springtime evolution of stratospheric ozone and circulation patterns over Svalbard archipelago in 2019 and 2020

David Tichopád[1*], Kamil Láska[1], Klára Čížková[1,2], Boyan H. Petkov[3,4]

[1]*Masaryk University, Faculty of Science, Department of Geography, Kotlářská 2, 611 37 Brno, Czech Republic*
[2]*Solar and Ozone Observatory, Czech Hydrometeorological Institute, Hradec Králové, 500 08, Czech Republic*
[3]*Department of Advanced Technologies in Medicine & Dentistry, University G. d'Annunzio, Chieti-Pescara, Italy*
[4]*Institute of Polar Sciences, National Research Council, Bologna, Italy*

Abstract

The polar vortex was exceptionally intense and persistent in late winter and spring 2020. The unusually cold lower stratosphere subsequently enabled ozone depletion over the Arctic. The behaviour of ozone layer and stratospheric parameters at the Ny-Ålesund station in the late winter and spring 2019 and 2020 were compared to each other by using reanalysed data, ground- and satellite-based observations and radiosonde measurement. The analyses based on the above-mentioned approaches confirmed a close relationship between ozone depletion and stratospheric circulation in 2020, when a strong polar vortex was observed, while in the case of the much weaker 2019 polar vortex such a relationship was insignificant. The deepest ozone decrease was found to occur at the end of March and in the first half of April 2020 at the 100–40 hPa pressure levels.

Key words: stratospheric ozone, stratospheric circulation, polar vortex, Svalbard archipelago

DOI: 10.5817/CPR2023-2-21

Received December 29, 2023, *accepted* January 22, 2024.
[*]Corresponding author: D. Tichopád <david.tichopad@mail.muni.cz>
Acknowledgements: This research was funded by the projects 'Czech Antarctic Research Programme 2023', Ministry of Education, and the project of Masaryk University 'MUNI/A/1469/2023'. The authors would also like to acknowledge the NASA Global Modeling and Assimilation Office for providing the MERRA-2 total ozone column and potential vorticity data reanalysis, and the European Centre for Medium-Range Weather Forecasts (ECMWF) for supplying data on stratospheric ozone mass mixing ratio, temperature, geopotential height, and potential vorticity. Additionally, the authors extend their acknowledgment to the Network for the Detection of Atmospheric Composition Change (NDACC) for providing data on the vertical distribution of ozone at the Ny-Ålesund station and Tropospheric Emission Monitoring Internet Service (TEMIS) for satellite measurements data of total ozone column at Ny-Ålesund. The authors thank an anonymous reviewer for constructive and useful comments.

***Abbreviations*:** DU – Dobson units, ECMWF – European Center for Medium-Range Weather Forecasts, ERS – Earth Remote-Sensing, ESRI – Environmental Systems Research Institute, GOME – Global Ozone Monitoring Experiment, GUV – Ground-based Ultraviolet, MERRA – Modern-Era Retrospective Analysis for Research and Applications, NASA – National Aeronautics and Space Administration, NDACC – Network for the Detection of Atmospheric Composition Change, ODS – Ozone-depleting substances, PSC – Polar stratospheric cloud, PVU – Potential vorticity unit, SSW – Sudden stratospheric warming, TEMIS – Tropospheric Emission Monitoring Internet Service, TOC – Total ozone column, UV – Ultraviolet radiation, WMO – World Meteorological Organization

Introduction

Stratospheric ozone is an important atmospheric gas, which helps to protect human health, surface ecosystems, and global climate in general (McKenzie et al. 2011). This is owing to its ability to absorb solar ultraviolet (UV) radiation and its conversion into thermal energy in the stratosphere. Since the 1970s, stratospheric ozone depletion in the Antarctic has been occurring periodically during the austral spring, primarily due to anthropogenic emissions of chlorofluorocarbons and another ozone depleting substances (Farman et al. 1985). As a result of the successful Montreal Protocol, Antarctic ozone layer has started recovering in recent years (Solomon et al. 2016, Kuttippurath and Nair 2017, Pazmiño et al. 2018, Weber et al. 2022). The recovery of the ozone layer in the Arctic is more challenging than in the Antarctic due to strong interannual variability of atmospheric dynamics at northern high latitudes (Langematz 2018). It may be further hindered by the ongoing climate change, which causes stratospheric cooling, and accompanied by moisture increase, create more favourable conditions for the formation of polar stratospheric clouds (PSCs) during spring period (von der Gathen et al. 2021). The higher occurrence of PSCs leads to an increase in chemical ozone depletion via the catalysation of various heterogeneous reactions on the cloud particles (Rex et al. 2002).

The main feature of the atmospheric circulation over the polar regions is the formation of a huge vortex, which is the strongest during winter. The Arctic and Antarctic polar vortices play a key role in the depletion of stratospheric ozone and the development of the annual ozone hole because they promote extremely low stratospheric temperatures, which may lead to the formation of PSCs (Solomon 1999, Newman 2010). The ozone depletion area depends on the strength and persistency of the polar vortex during spring (Solomon et al. 1986, Solomon 1999, Newman et al. 2004). Compared to the Southern Hemisphere, the Northern Hemisphere polar vortex is weaker due to more frequent dynamical disturbances. They are caused by stronger vertically propagating planetary waves, which are generated by relatively larger orographic obstacles and greater land-ocean contrasts compared to the Southern Hemisphere (Waugh and Randel 1999). The disruption of the Arctic polar vortex causes large interannual variability, including events known as sudden stratospheric warmings (SSWs). A SSW event involves a rapid increase in stratospheric air temperatures of up to 50°C in a few days (Baldwin et al. 2021). As a result of the weaker Arctic polar vortex, significant ozone depletion in the northern polar area occurs only occasionally and with variable intensity during winter and spring season

(Solomon et al. 2007). However, in the last few decades, several episodes of unusually stable Arctic polar vortices reminiscent of the Antarctic occurred in the spring of 1993, 1996, 1997, 2000, 2005, 2011, and 2020 (Manney et al. 1994, Hauchecorne et al. 2002, Koch et al. 2004, WMO 2007[6], Rösevall et al. 2008, Arnone et al. 2012). Extremely strong episodes were reported for the spring of 1997, 2011, and 2020 (Coy et al. 1997, Manney et al. 2011, 2020; Lawrence et al. 2020).

In 2011, a persistent polar vortex in the stratosphere caused an unusually long cold spell that lasted until the end of March, allowing PSCs to occur continuously for more than 100 days (Manney et al. 2011). A strong polar vortex in the spring of 2020 exhibited very similar behaviour to that of 2011, fulfilling the conditions for ozone layer destruction as well (Petkov et al. 2023).

The aim of this study is to compare ozone layer dynamics and stratospheric circulation over the Arctic Svalbard Archipelago in two contrasting spring periods. The first period covers the late winter and spring months of 2019 characterized by weak polar vortex and no ozone depletion. On the contrary, in the 2020 period, a widespread ozone depletion due to an unprecedentedly strong polar vortex was observed. In our study, the comparison is based on an assessment of linkages between ozone depletion and stratospheric circulation.

Data and Methods

Study area

The Ny-Ålesund station (78° 56′ N, 11° 56′ E) is located on the Brøgger Peninsula in the proximity of the Kongsfjorden Bay shore on the Spitsbergen Island, which is the largest island in the Svalbard Archipelago (Fig. 1). The archipelago is situated between the Arctic Ocean, the Barents Sea and the Greenland Sea, approximately between 74° – 81° N and 10° – 34° E. The area can be affected by both the cold Arctic air masses from the north and warmer, moist masses from the south. This atmospheric convergence induces the formation of pressure troughs, contributing to meteorological variability and fluctuations in weather patterns (Torkildsen 1984). At the Ny-Ålesund site, there are eighteen research institutions from eleven countries, with five maintaining a year-round presence. These institutions focus on environmental and earth sciences, utilizing the town's strategic location, pristine nature, and mild climate.

Data sources

The assessment of total ozone column (TOC) at Ny-Ålesund station in the period 2001–2020 was compiled satellite ozone observation (2001–2008) and ground-based measurements (2008–2020). The TOC satellite overpass data provided by the Global Ozone Monitoring Experiment (GOME) sensor were retrieved for the Ny-Ålesund station (Antón et al. 2011, TEMIS 2004[5]). The GOME sensor was installed on board of the second European Earth Remote-Sensing Satellite (ERS-2). Ground-based ozone observations at Ny-Ålesund were obtained from the narrow band filter radiometer UV-RAD, which was developed for the UV irradiance and TOC monitoring in the polar regions (Petkov et al. 2006).

For the purpose of spatial analysis, reanalysed data of TOC, ozone mass mixing ratio, geopotential height, and potential vorticity at the 50 hPa pressure level from the Modern-Era Retrospective Analysis for Research and Applications (MERRA-2) were used (Knowland et al. 2017, NASA 2023a[2]). The resolution for this dataset is 0.500 × 0.625°. For the assessment of ozone mass mixing ratio, temperature, geopotential height and potential vorticity at the 50 hPa pressure level at Ny-Ålesund, the ERA5 reanalysis from the European Center for Medium-Range Weather Forecasts (ECMWF 2023[1]) was utilized. The resolution of this dataset is 0.25 × 0.25°. The vertical profiles of ozone and temperature were obtained from sounding measurement of the Network for the Detection of Atmospheric Composition Change (NDACC), performed directly at the Ny-Ålesund station (NASA 2023b[3]).

The dependence of the daily anomaly of the ozone mass mixing ratio at 50 hPa on other stratospheric parameters (such as daily anomaly of temperature, geopotential heights, and potential vorticities at 50 hPa) was assessed using Spearman's correlation coefficient (Pruscha 2012). The nonparametric correlation coefficient based on the Shapiro-Wilk test of the data normality that indicate an asymmetric distribution of the data (Pruscha 2012) was also used in the analyses. All statistical analyses were carried out at the 0.05 level of significance using the ggpubr library in R programming (Kassambara 2022[8]). The processing of map outputs was performed using the ArcGIS Pro software (ESRI 2023[7]), and the graphical outputs were generated in the R programming language using the ggplot2 library (Wickham 2010[9]).

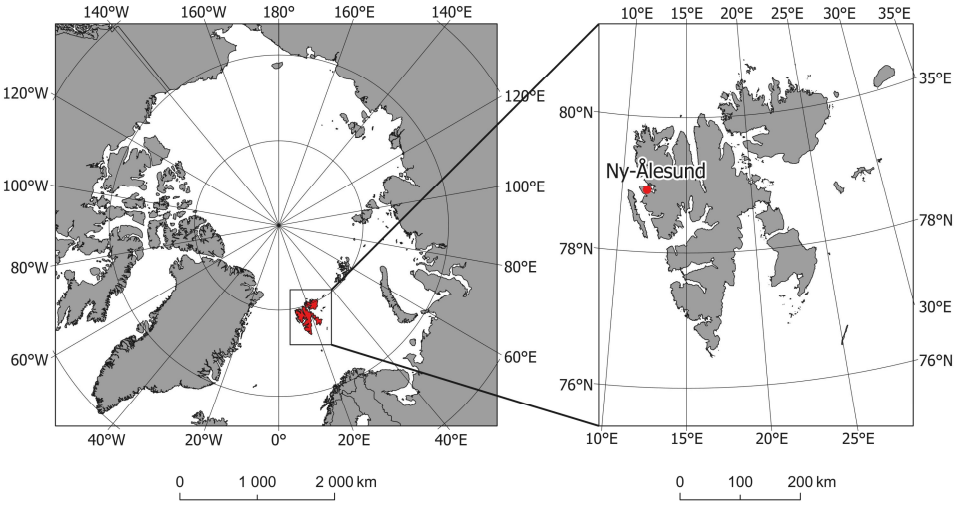

Fig. 1. Location of Ny-Ålesund station and Svalbard archipelago in the Arctic region (adapted from Norwegian Polar Institute 2023[4]).

Results

Seasonal variability of TOC from satellite and ground-based observations at Ny-Ålesund station in the period 2001–2020 is presented in Fig. 2. Fifteen-day moving means reach the highest values (~380–410 DU) in March and April, and then gradually decrease from 380 DU to 280 DU in late summer. In autumn, the moving means are maintained in the range of 270–290 DU. The standard deviation shows the highest interannual variability (20–50 DU) in the spring period.

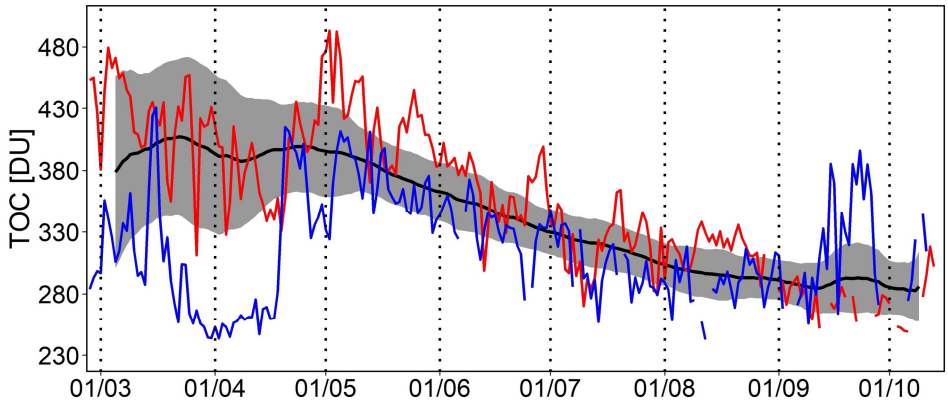

Fig. 2. Variability of total ozone column (TOC) at the Ny-Ålesund station compiled using satellite and ground-based observations: the 2001–2020 moving mean (black line) supplemented with standard deviation (grey area), and the daily TOC evolution in 2019 (red line) and 2020 (blue line).

Fig. 2 shows the distinct variation in daily mean TOC in 2019 and 2020 in relation to the long-term mean. In the spring of 2020, a dramatic drop in TOC below the long-term mean was observed, whereas in the spring of 2019, TOC consistently remained within or close to ± 1 standard deviation from the 2001–2020 running mean. The most significant decrease in TOC (more than 2σ) occurred at the end of March and the first half of April 2020, when the TOC was mostly in the range of 240–255 DU. The TOC rapidly increased by ~120 DU on April 19, returning to its long-term mean.

The spatial distribution of TOC and the position of the polar vortex represented by potential vorticity at 50 hPa in the region over the Arctic on 16 and 20 April 2020 can be seen in Fig. 3. Between these days, a recovery of the ozone layer at Ny-Ålesund was observed due to change in the stratospheric circulation and subsequent breaking up of the polar vortex. On April 16th, the ozone depletion area was situated over the Franz Josef Land, well corresponding to the position of the polar vortex. Over next four days, the polar vortex was disrupted and split on April 20th. One circulation core moved over Canada, while the other moved over Siberia. The break-up of the polar vortex allowed the advection of ozone rich air masses from lower latitudes, leading to a sharp increase in TOC by ~120 DU between April 16th and 20th.

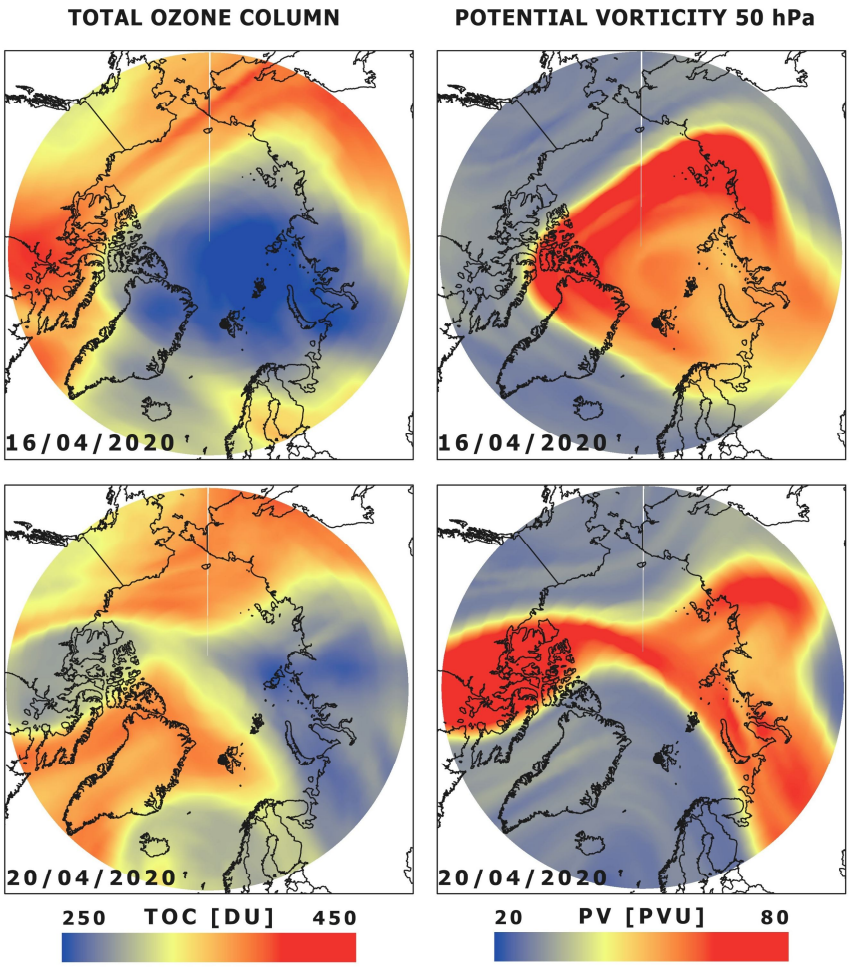

Fig. 3. Total ozone column (TOC; left panels) and potential vorticity (PV; right panels) over the Arctic on April 16 and 20, 2020.

Ozone mass mixing ratio and thermodynamical stratospheric parameters such as temperature, geopotential height and potential vorticity at 50 hPa in late winter and spring of 2019 and 2020 at Ny-Ålesund are summarized in Fig. 4. In the reference period 2001–2020, the ozone mass mixing ratio varied between ~$5 \cdot 10^{-6}$ – $6 \cdot 10^{-6}$ kg·kg^{-1} (Fig. 4a). However, during the 2020 spring, there was a sudden drop of the ozone mass mixing ratio below the long-term mean, with the lowest values (~$2 \cdot 10^{-6}$ kg·kg^{-1}) occurring at the end of March and first half of April 2020. This decrease exceeded 2σ, which was ~$3.5 \cdot 10^{-6}$ kg·kg^{-1} less than the long-term mean. The variation in the ozone mass mixing ratio differed during the spring of 2019, when values close to the long-term mean were observed.

In the late winter and spring of 2020, the temperature at 50 hPa was more than one standard deviation lower than the 2001 – 2020 mean. During the turn of March and

April 2020, the temperature was approximately 15 K below the long-term mean, causing photochemical depletion of ozone, which is well visible in Fig. 4a. The temperature reached mean values (215 K) in the second half of April 2020 (Fig. 4b). This increase of temperature corresponded with the breakup of the polar vortex (Fig. 3). In late of winter and spring 2019, the temperature variation was predominantly within the boundaries of one standard deviation from the long-term mean.

The evolution of geopotential height at 50 hPa during the late winter and spring was very similar to the temperature variation (Fig. 4c). The geopotential height in the 2020 was below the long-term mean until the second half of April 2020 when the polar vortex breakup occurred. The low geopotential height at 50 hPa indicated low air temperatures therefore the presence of the polar vortex. During the most significant ozone depletion at the turn of April and March, the geopotential height was ~800 m below the long-term mean. In the late winter and spring 2019, the geopotential height fluctuated around the long-term mean.

The potential vorticity variation at 50 hPa during late winter and spring of 2019 and 2020 at the Ny-Ålesund station, supplemented with the long-term mean and standard deviation, shows the highest potential vorticity was found in March and the first half of April 2020, with values of 15–30 PVU above the long-term mean (Fig. 4d). These conditions indicated the presence of the polar vortex above Ny-Ålesund, causing a decrease of stratospheric temperature and ozone depletion occurrence. The gradual decrease in potential vorticity observed during the second half of April 2020 indicated a weakening polar vortex. In general, the low potential vorticity in late winter and spring 2019, which is mostly below the long-term mean, signified a weak polar vortex.

The dependence of the ozone mass mixing ratio on thermodynamic parameters in the stratosphere, such as temperature, geopotential height, and potential vorticity at 50 hPa in late winter and spring of 2019 and 2020, is summarized in Fig. 5. These selected parameters are presented using daily anomalies with respect to the 2001 – 2020 reference period. The Spearman correlation coefficient (r_{sp} = 0.74) indicates a significant positive relationship between ozone mass mixing ratio and the temperature anomaly in late winter and spring of 2020 (Fig. 5a). A weak but statistically significant negative correlation (r_{sp} = -0.28) between the ozone mass mixing ratio and temperature at 50 hPa was observed in late winter and spring of 2019. The correlation between ozone mass mixing ratio and geopotential height at 50 hPa was significantly positive (r_{sp} = 0.82) in late winter and spring of 2020, but during the 2019 period, a moderately negative correlation (r_{sp} = -0.51) was observed (Fig. 5b). A different situation was observed between ozone mass mixing ratio and the potential vorticity at 50 hPa (Fig. 5c). The significant negative correlation (r_{sp} = -0.68) between ozone mass mixing ratio and potential vorticity was found in late winter and spring of 2020, while a weak, statistically insignificant positive correlation (r_{sp} = 0.12) occurred in late winter and spring 2019.

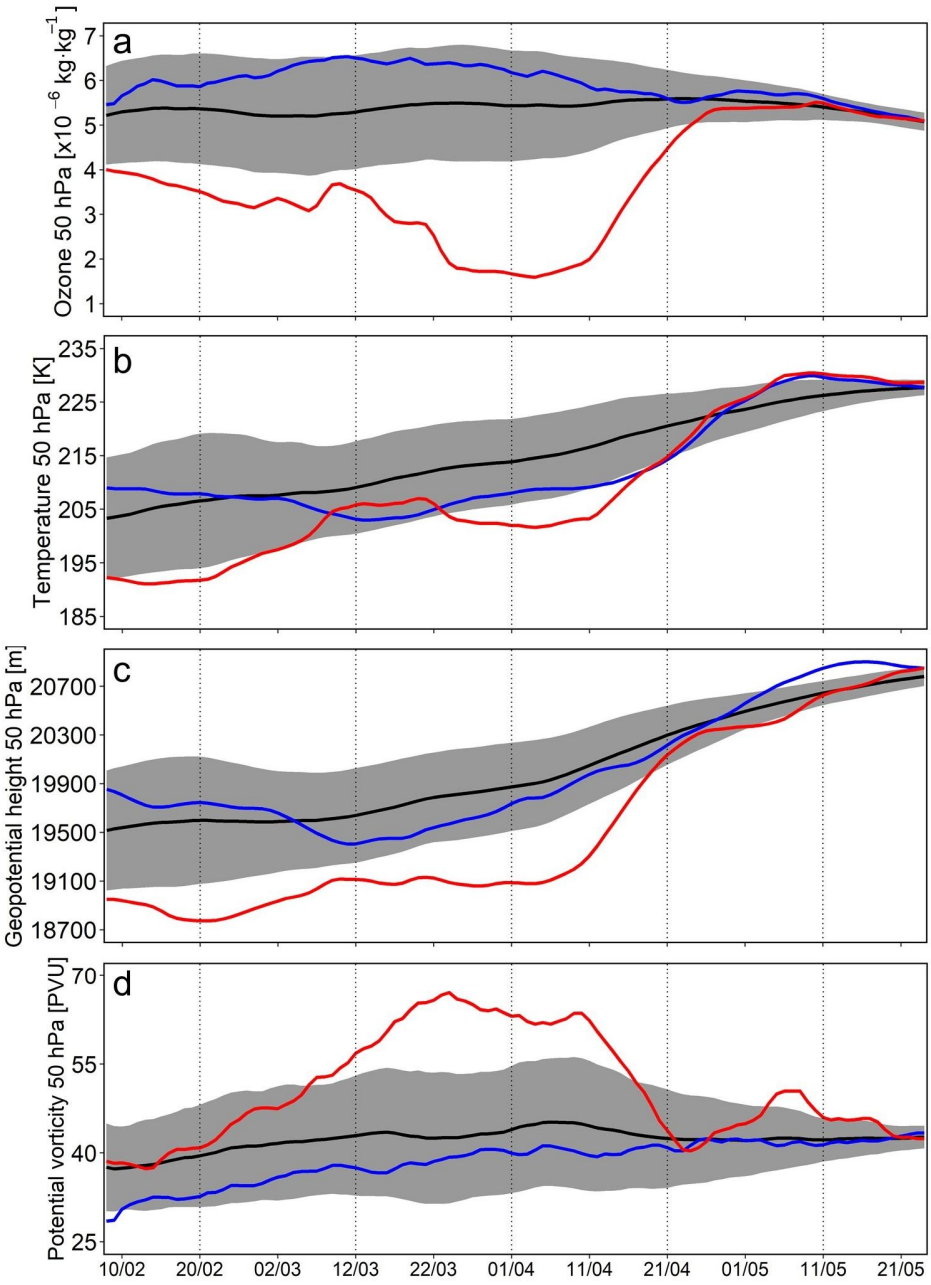

Fig. 4. Ozone mass mixing ratio (a), temperature (b), geopotential height (c) and potential vorticity (d) at the 50 hPa pressure level, based on ERA5 reanalysis data in late winter and spring 2019 (blue line) and 2020 (red line) supplemented with the mean (black line) and standard deviation (grey area) for the 2001–2020 reference period at the Ny-Ålesund station.

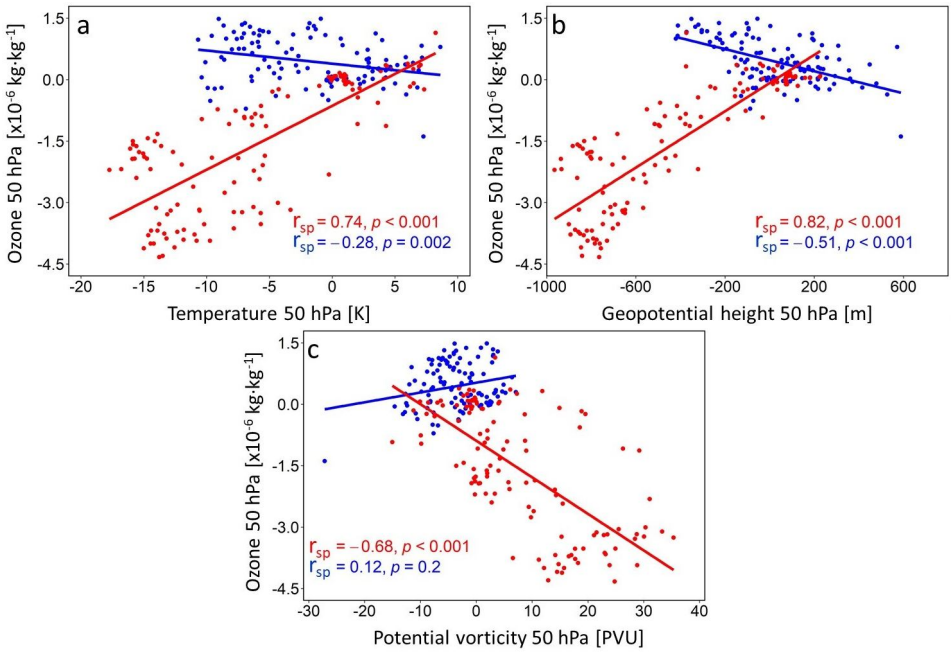

Fig. 5. Relationship between ozone mass mixing ratio at the 50 hPa pressure level and temperature (a), geopotential height (b) and potential vorticity (c) at the 50 hPa pressure level at the Ny-Ålesund station in late winter and spring 2019 (blue) and 2020 (red), supplemented by the Spearman correlation coefficient (r_{sp}) with the specified p-value (p). The parameters are expressed as anomalies with respect to the 2001–2020 reference period.

The evolution of daily mean of the ozone mass mixing ratios at 50 hPa within the latitudinal range of 60 – 90°N during late winter and spring 2019 and 2020 is expressed in Fig. 6. In the context of 2019, no ozone depletion was observed, and the ozone mass mixing ratio at 50 hPa remained approximately constant at $6 \cdot 10^{-6}$ kg·kg^{-1}. The minor variations observed during this period were attributed to the inherent natural variability of the Arctic ozone layer.

Conversely, a different situation occurred during the late winter and spring of 2020, when a severe ozone depletion was observed over the Arctic region, extending as far as Ny-Ålesund. As depicted in Fig. 6, ozone depletion was related to the meridional advection, indicating the transport of ozone-depleted air masses from the Arctic to 60°N. Notably, three significant advection events were identified during this period. The first event was recorded in early February 2020, followed by a second event at the end of February 2020. The most notable of these advection events occurred in late March and the first half of April 2020, when the ozone mass mixing ratio dropped to approximately $2 \cdot 10^{-6}$ kg·kg^{-1}, marking a difference of $4 \cdot 10^{-6}$ kg·kg^{-1} compared to the 2019 spring period. In the second half of April 2020, the ozone depletion shifted away from Ny-Ålesund. As a result, a subsequent ozone recovery was observed over Ny-Ålesund, leading to an increase in the ozone mass mixing ratio to $5 \cdot 10^{-6}$ kg·kg^{-1}. During May 2020, the ozone layer returned to the long-term mean.

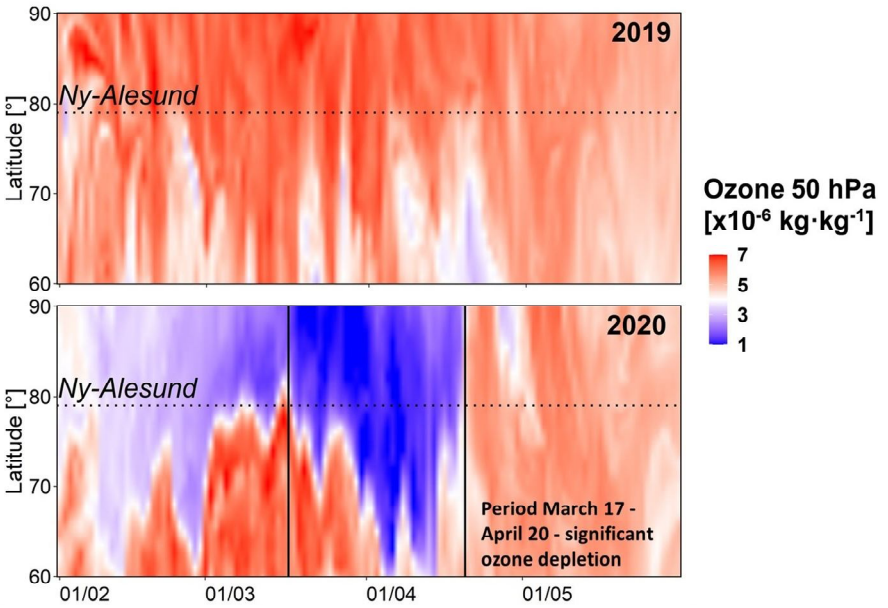

Fig. 6. Daily means of ozone mixing ratio at the 50 hPa pressure level in late winter and spring of 2019 and 2020 in the Northern subpolar and polar latitudes. Horizontal dotted line indicates the latitude of the Ny-Ålesund station. The black vertical lines in the lower panel mark the period with a significant ozone loss (March 17th – April 20th).

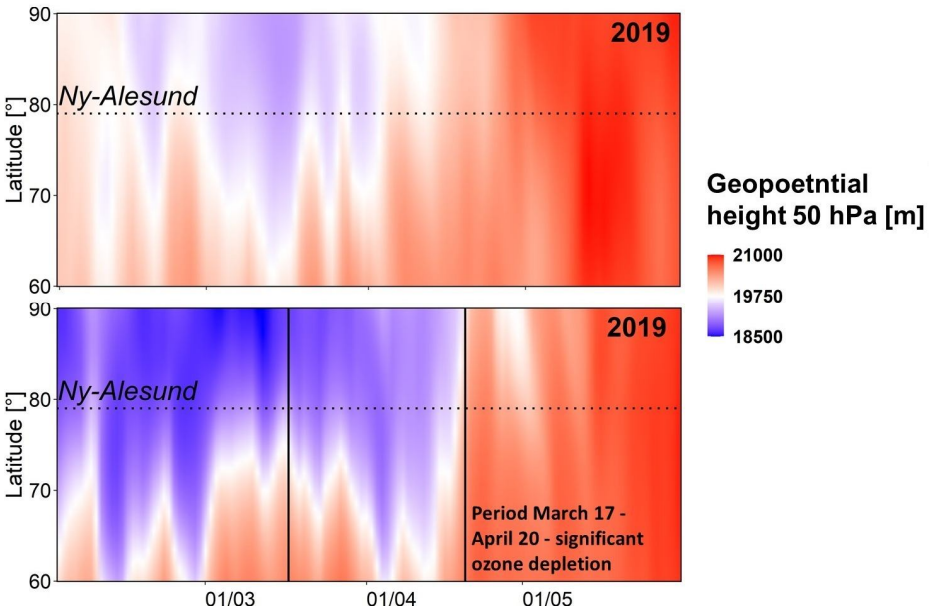

Fig. 7. Daily mean of geopotential height at 50 hPa pressure level in late winter and spring of 2019 and 2020 in the Northern subpolar and polar latitudes. Horizontal dotted line indicates the latitude of the Ny-Ålesund station. The black vertical lines in the lower panel mark the period with a significant ozone loss (March 17th – April 20th).

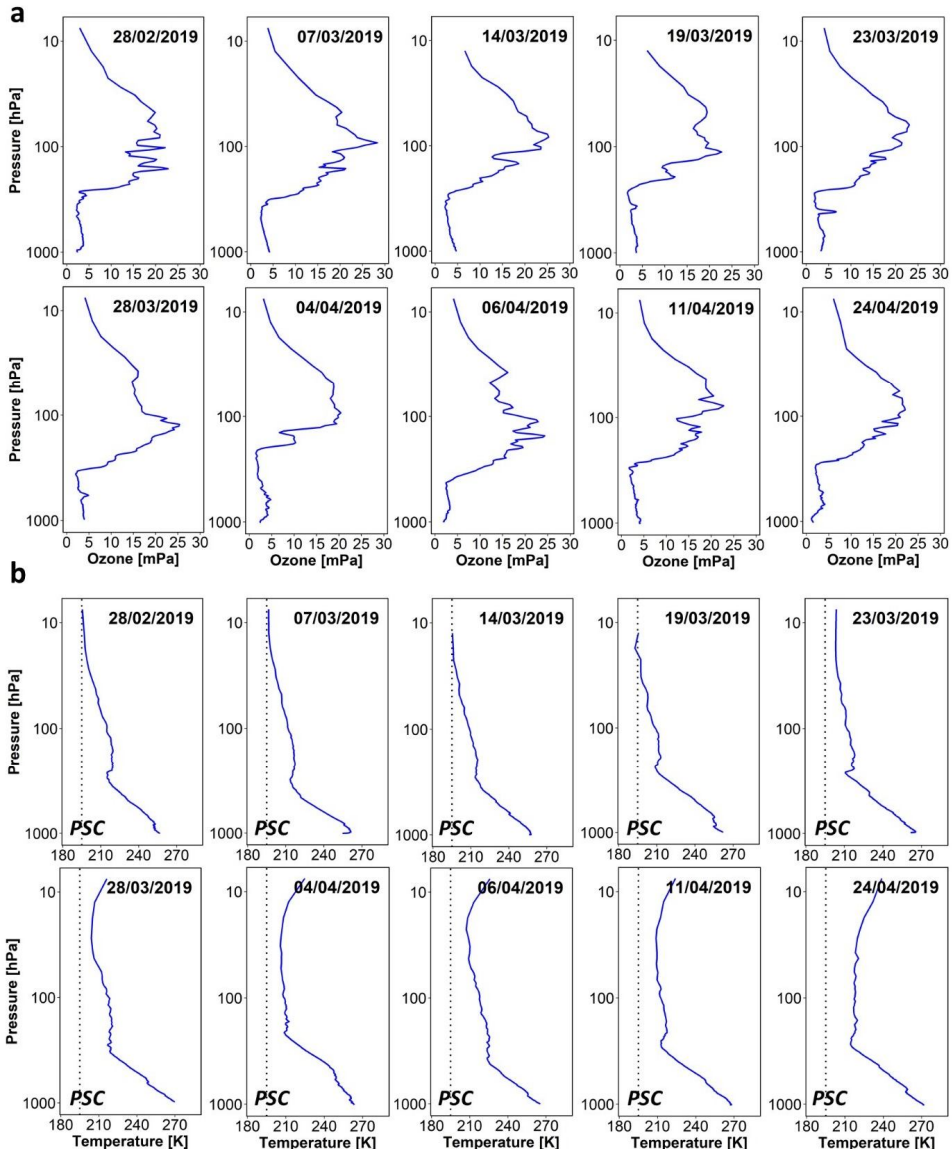

Fig. 8. Selected vertical profiles of ozone (a) and temperature (b) at the Ny-Ålesund station during late winter and spring of 2019. The temperature for PSC-1 formation (195 K) is indicated by the dotted line.

Fig. 7 shows the progression of daily mean geopotential height at 50 hPa within the latitudinal range of 60–90°N during late winter and spring of 2019 and 2020. In 2019, a weak polar vortex, denoted by a lower geopotential height, was discernible. In March 2019, the weak polar vortex shifted over Ny-Ålesund, without instigating any ozone depletion (Fig. 6). Compared to 2019, the polar vortex and geopotential height pattern during the late winter and spring of 2020 were significantly different. The observed pattern of low geopotential heights extending to subpolar re-

gions align with the periods of ozone-depleted air advection (Fig. 6). The influx of ozone-depleted air masses into lower latitudes was linked to the expansion of the polar vortex towards the southern parts of Europe. The increased in geopotential heights observed in late April and May 2020 indicated the disintegration of the polar vortex.

The radiosonde measurements of ozone vertical profiles available at Ny-Ålesund during late winter and spring 2019 can be seen in Fig. 8a. In 2019, no significant decrease in ozone was observed in the vertical distribution. The highest ozone partial pressure (~25 mPa), was consistently recorded at 100 hPa. These ozone amounts corresponded to the vertical temperature profiles, which always exceeded the temperature threshold (195 K) required for PSC formation (Fig. 8b). At 100 hPa, the temperature ranged between 210 and 220 K.

At the end of February 2020 (Fig. 9a), the highest partial pressure of ozone (~15 mPa at 100 hPa) was approximately 10 mPa lower compared to February 2019. At the beginning of March 2020, ozone depletion started to develop at 50 hPa. The most significant ozone decrease occurred in the first half of April 2020, when the ozone amount at 50 hPa dropped to ~2 mPa (~15 mPa less than in the first half of April 2019). The recovery of the ozone layer (Fig. 9a) was observed in the second half of April 2020.

The decrease of ozone at 50 hPa in late winter and spring 2020 corresponded to the changes in temperature vertical profiles (Fig. 9b). The most significant drop in temperature occurred at the end of March and during first half of April 2020, when temperatures at 50 hPa dropped to 195–200 K. These temperatures, approximately 15–20 K lower than in the 2019, indicating that PSCs may have formed over Ny-Ålesund.

Discussion

The results indicate a different evolution of TOC at Ny-Ålesund in the late winter and spring of 2019 and 2020. A sudden decrease of TOC, which accounted for more than 2σ in comparison with the reference period 2001–2020, was observed at the end of March and the first week of April 2020. These results are consistent with the findings reported by Svendby et al. (2021), who analysed ground-based observations of the GUV radiometer at Ny-Ålesund. The mean TOC in February to April 2020 was the lowest since the beginning of satellite measurements in 1979 (Svendby et al. 2021). Also Lawrence et al. (2020) concluded that TOC over the Arctic region was unprecedentedly low in late winter and spring of 2020. This ozone depletion event was mainly caused by a persistent polar vortex, which provided suitable conditions for chemical ozone depletion due to low temperatures (Manney et al. 2020, Wohltmann et al. 2020, Grooß and Müller 2021). The strong polar vortex could also cause ozone depletion at a local level, such as the Ny-Ålesund station.

The presence of a strong polar vortex in 2020 was confirmed by lower temperature, geopotential height and potential vorticity compared to the long-term 50 hPa values over the Ny-Ålesund station. The most significant ozone depletion at 50 hPa occurred in late March and early April due to the ongoing photochemical reactions and advection of ozone-poor air from higher latitudes. The final breakdown of the polar vortex occurred between April 16th – 20th, 2020. On April 16th, the polar vortex was still extended over Siberia and part of Arctic Ocean. In the following days, the polar vortex split into two circulation cores and shifted from Ny-Ålesund above the Laptev sea, as an effect of the advection of ozone rich air from lower latitudes.

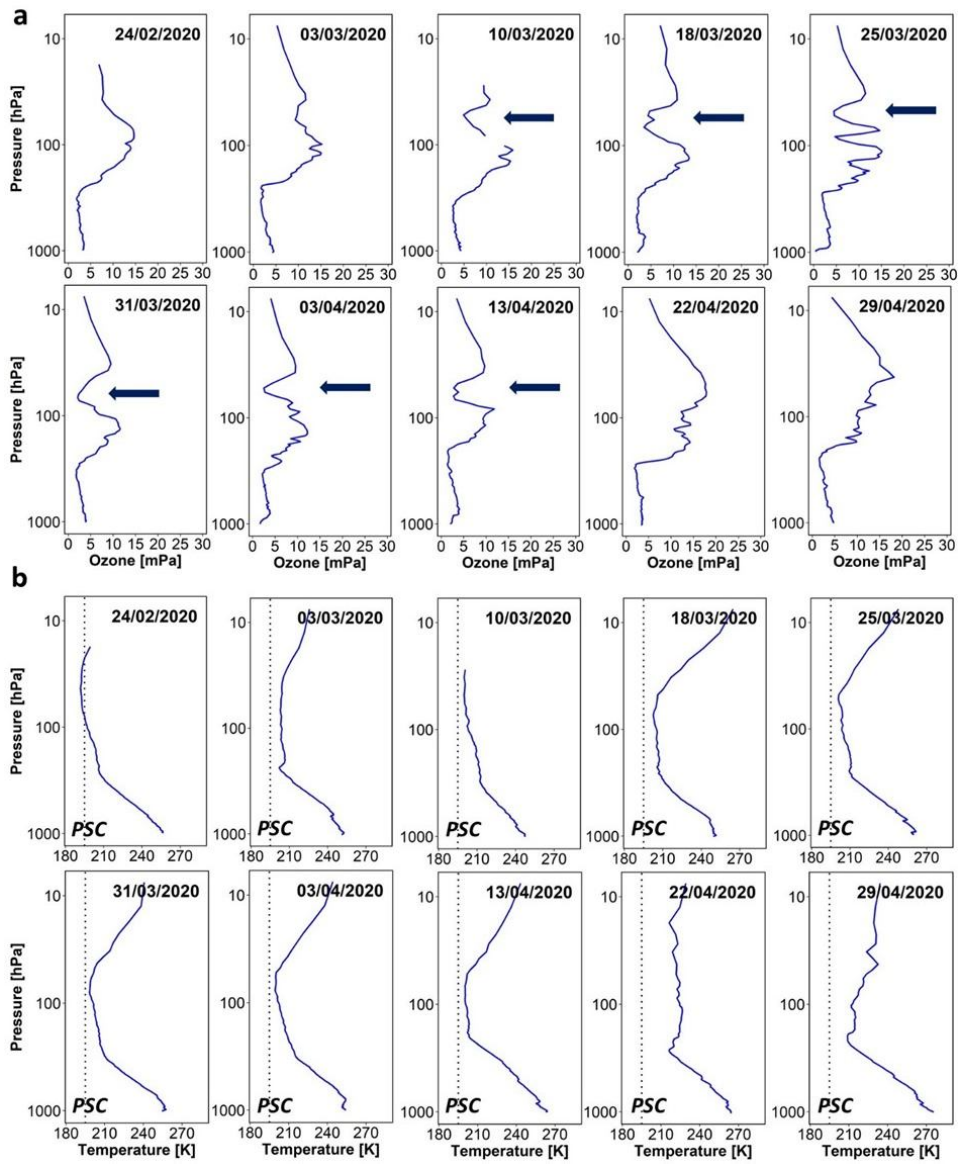

Fig. 9. Selected vertical profile of ozone (a) and temperature (b) at the Ny-Ålesund station during late winter and spring of 2020. The temperature for PSC-1 formation (195 K) is indicated by the dotted line. The blue arrow shows the occurrence of ozone depletion.

The dependence between the ozone depletion on stratospheric circulation at 50 hPa for the Ny-Ålesund station was stronger in late winter and spring 2020 than in 2019. During strong polar vortex events, a close dependence between stratospheric ozone and circulation over Ny-Ålesund, leading to ozone depletion over the Arctic, has been registered. On the contrary, during the periods of a weaker polar

vortex, this dependence is lower or even reserved. The stronger relationship between ozone amounts and stratospheric parameters, particularly temperature, in 2020 was caused by the drop of temperatures below the threshold of 195 K, leading to the PSCs formation and chemical ozone depletion. Moreover, ozone depletion during the spring season is intensified by a positive feedback loop, in which low temperatures play a role and contributes to ozone depletion that then causes further radiative cooling of the stratosphere and therefore even faster ozone losses (Randel and Wu 1999). The second type of feedback mechanism is associated with the dynamical transport of ozone from the tropical photochemical source region to high latitudes, where the intense and persistent polar vortex hinders the transport of ozone to polar regions (Randel and Wu 1999). For instance, the anomalously strong Arctic vortex in the spring of 1997 was a primary factor of the observed low polar ozone (Manney et al. 1997). In spring 2019, the weak, negative but significant correlation between ozone mass mixing ratio and temperature at 50 hPa was caused by the advection of relatively warmer, ozone-poorer air masses from lower latitudes (Fuxiang et al. 2018).

The dependence of stratospheric ozone on the polar vortex characteristics in the Arctic during late winter and spring of 2020 was confirmed using geopotential height. In case of a stronger polar vortex, lower stratospheric ozone corresponded to the lower geopotential height. Compared to previous months, greater ozone depletion occurred at Ny-Ålesund around the turn of March and April 2020 due to increased photochemical activity (Harris et al. 2010). In spring 2019, temperatures did not drop below the threshold of 195 K and the variability of stratospheric parameters had no major impact on the ozone layer.

The variation in the ozone amounts studied by radiosonde measurements carried out at Ny-Ålesund confirmed that the most pronounced ozone depletions (1.86 mPa) occurred on 13 April 2020 at pressure levels ranging from 100 to 40 hPa. This was well linked with the lowest temperatures (200 – 205 K) observed at the same pressure levels. Although the spring 2020 stratospheric temperatures at Ny-Ålesund were above 195 K, chemical ozone depletion occurred in the central part of the polar vortex (Lawrence et al. 2020, Manney et al. 2020). Ozone-depleted air masses were advected over Ny-Ålesund from the region of its chemical depletion during the displacement of the polar vortex toward Europe (Petkov et al. 2023). Furthermore, ozone depletion was significantly enhanced by the strong polar vortex, which serves as a barrier in the transport of ozone from the tropics to the polar regions. Thus it impedes the Brewer-Dobson circulation, causing a dynamically conditioned ozone loss (Strahan et al. 2013). In the late winter and spring of 2019, ozone distribution between 100 and 40 hPa was approximately 20 mPa higher compared to 2020. Ozone sonde measurements at various locations in the Arctic during the spring of 2020 indicated that the observed minima in the vertical ozone profiles were comparable to those in the Antarctic ozone hole (Wohltmann et al. 2020).

Temperature data available for the 2019 –2020 winter season (ECMWF 2023[1]) support the trend of decreasing stratospheric winter temperature reported by Wohltmann et al. (2020), von der Gathen et al. (2021). Colder conditions in the winter and spring Arctic stratosphere cause a higher probability of ozone depletion events (Tilmes et al. 2006, von der Gathen et al. 2021). In future, high interannual variability but a more frequent occurrence of cold stratospheric winters are likely to happen (von der Gathen et al. 2021). It is predicted that the decline of anthropogenic ozone-depleting substances (ODS) will lead to the recovery of the ozone layer within a few decades, but the large interannual variabil-

ity of winter temperatures in the Arctic stratosphere can reverse these effects in individual winters (Dhomse et al. 2018). Therefore, the future state of spring Arctic ozone layer will depend on the balance between initial stratospheric ozone concentrations at the beginning of the winter, ozone transport by the Brewer-Dobson circulation, and chemical ozone destruction, which is governed by a multitude of factors including the ODS concentration and stratospheric dynamics (von der Gathen et al. 2021).

Conclusion

In this study, an analysis of late winter and spring total ozone column in 2019 and 2020 at the Ny-Ålesund station was carried out based on ground- and satellite-based measurements. The analysis of stratospheric temperature, geopotential height, and potential vorticity at 50 hPa, based on the ERA5 reanalysis data, confirmed the intense and persistent polar vortex in late winter and spring of 2020 over the Ny-Ålesund station. The remarkably strong polar vortex caused a decrease in stratospheric ozone, especially at the turn of March and April 2020. The radiosonde measurements showed that the largest ozone losses in vertical profiles occurred at the end of March and in the first half of April 2020 from 100 to 40 hPa. During this period, there was a decrease in the total ozone column by more than two standard deviation (2σ). Stratospheric ozone has been shown to depend more strongly on stratospheric circulation parameters under strong polar vortex conditions than under weak polar vortex conditions.

The polar vortex is a dynamically developing system that can have an asymmetric shape and ozone depletion area consequently depends on its form and rotation. During the polar vortex breakup, ozone losses can be observed even in the mid-latitudes. The total ozone column decline then leads to an increase in harmful ultraviolet radiation on the Earth's surface. Ozone-depletion events may recur in future due to cooling in the stratosphere. For this reason, further research, observation and mathematical modelling of the Arctic polar vortex and ozone layer dynamics, are necessary.

References

ANTÓN, M., KROON, M., LÓPEZ, M., VILAPLANA, J. M., BAÑÓN, M., VAN DER A, R., VEEFKIND, J. P., STAMMES, P. and ALADOS-ARBOLEDAS, L. (2011): Total ozone column derived from GOME and SCIAMACHY using KNMI retrieval algorithms: Validation against Brewer measurements at the Iberian Peninsula. *Journal of Geophysical Research*, 116: D22303. doi: 10.1029/2011JD016436

ARNONE, E., CASTELLI, E., PAPANDREA, E., CARLOTTI, M. and DINELLI, B. M. (2012): Extreme ozone depletion in the 2010–2011 Arctic winter stratosphere as observed by MIPAS/ENVISAT using a 2-D tomographic approach. *Atmospheric Chemistry and Physics*, 12: 9149-9165.

BALDWIN, M. P., AYARZAGÜENA, B., BIRNER, T., BUTCHART, N., BUTLER, A. H., CHARLTON-PEREZ, A. J., DOMEISEN, D. I. V., GARFINKEL, C. I., GARNY, H., GERBER, E. P., HEGGLIN, M. I., LANGEMATZ, U. and PEDATELLA, N. M. (2021): Sudden stratospheric warmings. *Reviews of Geophysics*, 59.

COY, L., NASH, E. R. and NEWMAN, P. A. (1997): Meteorology of the polar vortex: Spring 1997. *Geophysical Research Letters*, 24: 2693-2696.

DHOMSE, S. S., KINNISON, D., CHIPPERFIELD, M. P., SALAWITCH, R. J., CIONNI, I., HEGGLIN, M. I., ABRAHAM, N. L., AKIYOSHI, H., ARCHIBALD, A. T., BEDNARZ, E. M., BEKKI, S., BRAESICKE, P., BUTCHART, N., DAMERIS, M., DEUSHI, M., FRITH, S., HARDIMAN, S. C., HASSLER, B., HOROWITZ, L. W., HU, R.-M., JÖCKEL, P., JOSSE, B., KIRNER, O., KREMSER, S., LANGEMATZ, U., LEWIS, J., MARCHAND, M., LIN, M., MANCINI, E., MARÉCAL, V., MICHOU, M., MORGENSTERN, O., O'CONNOR, F. M., OMAN, L., PITARI, G., PLUMMER, D. A., PYLE, J. A., REVELL, L. E., ROZANOV, E., SCHOFIELD, R., STENKE, A., STONE, K., SUDO, K., TILMES, S., VISIONI, D., YAMASHITA, Y. and ZENG, G. (2018): Estimates of ozone return dates from Chemistry-Climate Model Initiative simulations. *Atmospheric Chemistry and Physics*, 18: 8409-8438.

FARMAN, J., GARDINER, B. and SHANKLIN, J. (1985): Large losses of total ozone in Antarctica reveal seasonal ClOx/NOx interaction. *Nature*, 315: 207-210.

FUXIANG, H., SULING, R., SHUANGSHUANG, H., XIANGDONG, Z. and XUEJIAO, D. (2018): Spatiotemporal variations of the correlation between the Arctic atmospheric ozone and temperature. IGARSS 2018 – 2018 IEEE International Geoscience and Remote Sensing Symposium, Valencia, Spain: pp. 6544–6547.

GROOß, J.-U., MÜLLER, R. (2021): Simulation of record Arctic stratospheric ozone depletion in 2020. *Journal of Geophysical Research: Atmospheres*, 126.

HARRIS, N. R. P., LEHMANN, R., REX, M., and VON DER GATHEN, P. (2010): A closer look at Arctic ozone loss and polar stratospheric clouds. *Atmospheric Chemistry and Physics*, 10: 8499-8510.

HAUCHECORNE, A., GODIN, S., MARCHAND, M., HESSE, B. and SOUPRAYEN, C. (2002): Quantification of the transport of chemical constituents from the polar vortex to midlatitudes in the lower stratosphere using the high-resolution advection model MIMOSA and effective diffusivity. *Journal of Geophysical Research*, 107: 8289.

KNOWLAND, K. E., OTT, L. E., DUNCAN, B. N. and WARGAN, K. (2017): Stratospheric intrusion-influenced ozone air quality exceedances investigated in the NASA MERRA-2 reanalysis. *Geophysical Research Letters*, 44: 10691-10701.

KOCH, G., WERNLI, H., BUSS, S., STAEHELIN, J., PETER, T., LINIGER, M. A. and MEILINGER, S. (2004): Quantification of the impact in mid-latitudes of chemical ozone depletion in the 1999/2000 Arctic polar vortex prior to the vortex breakup. *Atmospheric Chemistry and Physics Discussions*, 4: 1911-1940.

KUTTIPPURATH, J., NAIR, P. J. (2017): The signs of Antarctic ozone hole recovery. *Scientific Reports*, 7: 585.

LANGEMATZ, U. (2018): Future ozone in a changing climate. *Comptes Rendus Geoscience*. 350: 403-409.

LAWRENCE, Z. D., PERLWITZ, J., BUTLER, A. H., MANNEY, G. L., NEWMAN, P. A., LEE, S. H. and NASH, E. R. (2020): The remarkably strong Arctic Stratospheric Polar Vortex of winter 2020: Links to record-breaking Arctic oscillation and ozone loss. *Journal of Geophysical Research: Atmospheres*, 125.

MANNEY, G. L., FROIDEVAUX, L., SANTEE, M. L., ZUREK, R. W. and WATERS, J. W. (1997): MLS observations of Arctic ozone loss in 1996–97. *Geophysical Research Letters*, 24: 2697-2700.

MANNEY, G. L., LIVESEY, N. J., SANTEE, M.L., FROIDEVAUX, L., LAMBERT, A., LAWRENCE, Z. D., MILLÁN, L. F., NEU, J. L., READ, W. G., SCHWARTZ, M. J. and FULLER, R. A. (2020): Record - low Arctic stratospheric ozone in 2020: MLS observations of chemical processes and comparisons with previous extreme winters. *Geophysical Research Letters*, 47.

MANNEY, G. L., SANTEE, M. L., REX, M., LIVESEY, N. J., PITTS, M. C., VEEFKIND, P., NASH, E. R., WOHLTMANN, I., LEHMANN, R., FROIDEVAUX, L., POOLE, L. R., SCHOEBERL, M. R., HAFFNER, D. P., DAVIES, J., DOROKHOV, V., GERNANDT, H., JOHNSON, B., KIVI, R., KYRÖ, E., LARSEN, N., LEVELT, P. F., MAKSHTAS, A., MCELROY, C. T., NAKAJIMA, H., PARRONDO, M. C., TARASICK, D. W., VON DER GATHEN, P., WALKER, K. A. and ZINOVIEV, N. S. (2011): Unprecedented Arctic ozone loss in 2011. *Nature*, 478: 469-475.

MANNEY, G. L., ZUREK, R. W., GELMAN, M. E., MILLER, A. J. and NAGATANI, R. (1994): The anomalous arctic lower stratospheric polar vortex of 1992–1993. *Geophysical Research Letters*, 21: 2405-2408.

McKenzie, R. L., Aucamp, P. J., Bais, A. F., Björn, L. O., Ilyasf, M. and Madronichg, S. (2011): Ozone depletion and climate change: Impacts on UV radiation. *Photochemical & Photobiological Sciences*, 10: 182-198.

Newman, P. A. (2010): Chemistry and dynamics of the Antarctic ozone hole. *In*: L. M. Polvani, A. H. Sobel, D. W. Waugh: The stratosphere: Dynamics, transport, and chemistry. *Geophysical Monograph Series*, 190: 43-57.

Newman, P. A., Kawa, S. R. and Nash, E. R. (2004): On the size of the Antarctic ozone hole. *Geophysical Research Letters*, 31.

Pazmiño, A., Godin-Beekmann, S., Hauchecorne, A., Claud, C., Khaykin, S., Goutail, F., Wolfram, E., Salvador, J. and Quel, E. (2018): Multiple symptoms of total ozone recovery inside the Antarctic vortex during austral spring. *Atmospheric Chemistry and Physics*, 18: 7557-7572.

Petkov, B. H., Vitale, V., Di Carlo, P., Drofa, O., Mastrangelo, D., Smedley, A. R. D., Diémoz, H., Siani, A. H., Fountoulakis, I., Webb, A. R., Bais, A., Kift, R., Rimmer, J., Casale, G. R., Hansen, G. H., Svendby, T., Pazmiño, A., Werner, R., Atanassov, A. M., Láska, K., Backer, H. D., Mangold, A., Köhler, U., Velazco, V. A., Stübi, R., Solomatnikova, A., Pavlova, K., Sobolewski, B. S., Johnsen, B., Goutail, F., Mišaga, O., Aruffo, E., Metelka, L., Tóth, Z., Fekete, D., Aculinin, A. A., Lupi, A., Mazzola, M. and Zardi, F. (2023). An unprecedented Arctic ozone depletion event during spring 2020 and its impacts across Europe. *Journal of Geophysical Research: Atmospheres*, 128.

Petkov, B. H., Vitale, V., Tomasi, C., Bonafé, U., Scaglione, S., Flori, D., Santaguida, R., Gausa, M., Hansen, G. and Colombo, T. (2006): Narrowband filter radiometer for ground-based measurements of global ultraviolet solar irradiance and total ozone. *Applied Optics*, 45: 4383-4395.

Pruscha, H. (2012): Statistical analysis of climate series: Analyzing, plotting, modeling, and predicting with R. Springer Science & Business Media.

Randel, W. J., Wu, F. (1999): A stratospheric ozone trends data set for global modeling studies. *Geophysical Research Letters*, 26: 3089-3092.

Rex, M., Salawitch, R. J., Harris, N. R. P., von der Gathen, P., Braathen, G. O., Schulz, A., Deckelmann, H., Chipperfield, M., Sinnhuber, B. M., Reimer, E., Alfier, R., Bevilacqua, R., Hoppel, K., Fromm, M., Lumpe, J., Küllmann, H., Kleinböhl, A., Bremer, H., von König, M., Künzi, K., Toohey, D., Vömel, H., Richard, E., Aikin, K., Jost, H., Greenblatt, J. B., Loewenstein, M., Podolske, J. R., Webster, C. R., Flesch, G. J., Scott, D. C., Herman, R. L., Elkins, J. W., Ray, E. A., Moore, F. L., Hurst, D. F., Romashkin, P., Toon, G. C., Sen, B., Margitan, J. J., Wennberg, P., Neuber, R., Allart, M., Bojkov, B. R., Claude, H., Davies, J., Davies, W., De Backer, H., Dier, H., Dorokhov, V., Fast, H., Kondo, Y., Kyrö, E., Litynska, Z., Mikkelsen, I. S., Molyneux, M. J., Moran, E., Nagai, T., Nakane, H., Parrondo, C., Ravegnani, F., Skrivankova, P., Viatte, P. and Yushkov, V. (2002): Chemical depletion of Arctic ozone in winter 1999/2000. *Journal of Geophysical Research: Atmospheres,* 107.

Rösevall, J. D., Murtagh, D. P., Urban, J., Feng, W., Eriksson, P., and Brohede, S. (2008): A study of ozone depletion in the 2004/2005 Arctic winter based on data from Odin/SMR and Aura/MLS. *Journal of Geophysical Research*, 113.

Solomon, S. (1999): Stratospheric ozone depletion' a review of concepts and history. *Reviews of Geophysics*, 37: 275-316.

Solomon, S., Garcia, R., Rowland, F. and Wuebbles, D. J. (1986): On the depletion of Antarctic ozone. *Nature*, 321: 755-758.

Solomon, S., Ivy, D. J., Kinnison, D., Mills, M. J., Neely III, R. R. and Schmidt, A. (2016): Emergence of healing in the Antarctic ozone layer. *Science*, 353: 269-274.

Solomon, S., Portmann, R. W. and Thompson, D. W. J. (2007): Contrasts between Antarctic and Arctic ozone depletion. *Proceedings of the National Academy of Sciences*, 104: 445-449.

Strahan, S. E., Douglass, A. R. and Newman, P. A. (2013): The contributions of chemistry and transport to low arctic ozone in March 2011 derived from Aura MLS observations. *Journal of Geophysical Research: Atmospheres*, 118: 1563-1576.

SVENDBY, T. M., JOHNSEN, B., KYLLING, A., DAHLBACK, A., BERNHARD, G. H., HANSEN, G. H., PETKOV, B. H. and VITALE, V. (2021): GUV long-term measurements of total ozone column and effective cloud transmittance at three Norwegian sites. *Atmospheric Chemistry and Physics*, 21: 7881-2021.

TILMES, S., MÜLLER, R., ENGEL, A., REX, M. and RUSSELL III, J. M. (2006): Chemical ozone loss in the Arctic and Antarctic stratosphere between 1992 and 2005. *Geophysical Research Letters*, 33.

TORKILDSEN, T. (1984): Svalbard: Vart Nordligste Norge. Oslo, Forlaget Det Beste.

VON DER GATHEN, P., KIVI, R., WOHLTMANN, I., SALAWITCH, R. J. and REX, M. (2021): Climate change favours large seasonal loss of arctic ozone. *Nature Communications*, 12: 3886.

WAUGH, D. W., RANDEL, W. J. (1999): Climatology of Arctic and Antarctic polar vortices using elliptical diagnostics. *Journal of the Atmospheric Sciences*, 56: 1594-1613.

WEBER, M., AROSIO, C., COLDEWEY-EGBERS, M., FIOLETOV, V. E., FRITH, S. M., WILD, J. D., TOURPALI, K., BURROWS, J. P. and LOYOLA, D. (2022): Global total ozone recovery trends attributed to ozone-depleting substance (ODS) changes derived from five merged ozone datasets. *Atmospheric Chemistry and Physics*, 22: 6843-6859.

WOHLTMANN, I., VON DER GATHEN, P., LEHMANN, R., MATURILLI, M., DECKELMANN, H., MANNEY, G. L., DAVIES, J., TARASICK, D., JEPSEN, N., KIVI, R., LYALL, N. and REX, M. (2020): Near-complete local reduction of Arctic stratospheric ozone by severe chemical loss in spring 2020. *Geophysical Research Letters*, 47.

Web sources / Other sources

[1] ECMWF (2023): European centre for medium-range weather forecasts, ERA-5 reanalyses. https://doi.org/10.24381/cds.adbb2d47

[2] NASA (2023a): Earthdata. Giovanni, https://giovanni.gsfc.nasa.gov/giovanni/

[3] NASA (2023b): Network for the Detection of Atmospheric Composition Change. https://www-air.larc.nasa.gov/missions/ndacc/data.html?station=ny.alesund/ames/o3sonde/

[4] Norwegian Polar Institute (2023): Norwegian Polar Institute Map Data and Services. https://geodata.npolar.no/

[5] TEMIS (2004): Valks, P.J.M., de Haan, J. F., Veefkind, J. P., van Oss R. F. and D.S. Balis, TOGOMI: An improved total ozone retrieval algorithm for GOME, XX Quadrennial Ozone Symposium, 1/6/2004-8/6/2004, C.S. Zerefos (Ed), Athens, University of Athens, pp. 129–130.

[6] WMO (2007): Scientific assessment of ozone depletion: 2006. Global ozone research and monitoring project – rep. 50. *World Meteorological Organization*.

Software

[7] ESRI (2023): ArcGIS Pro. https://www.esri.com/en-us/arcgis/products/arcgis-pro/overview

[8] KASSAMBARA, A. (2022): Ggpubr: 'Ggplot2' Based Publication Ready Plots. https://cran.r-project.org/web/packages/ggpubr/index.html

[9] WICKHAM, H. (2010): ggplot2: Elegant Graphics for Data Analysis. *Journal of Statistical Software*, 35.